Conference Paper, Published Version

Lim, Siow-Yong; Yu, Guoliang; Tan, Soon-Keat

Flow and Scouring in Main Channel due to Abutments

First International Conference on Scour of Foundations, ICSF-1
Texas A&M University, College Station, Texas, USA November 17-20, 2002

Flow and Scouring in Main Channel due to Abutments

By

Guoliang Yu[1] Siow-Yong Lim[2] and Soon-Keat Tan[2]

ABSTRACT

This paper presents the flow and scouring characteristics around a vertical-wall abutment spanning across the floodplain and terminates at the edge of the submerged floodplain of a two-stage channel. The vertical velocity profiles around the abutment in the main channel were measured using an ADV. It was found that the flow pattern consists of complex interactions of spiral vortices around the abutment, downflows towards the bed, and upflow eddies behind the abutment nose. The velocity profiles around the abutment follow the logarithmic law near the bed, but the boundary layer thickness increases as the scouring process progresses. The increase of the bed shear stress around the abutment depends on the approach discharge. For the flat bed condition, equivalent to the beginning of scouring, the maximum value of the bed shear stress measured around the abutment nose was 3.8 times compared to that at the upstream approach section. At equilibrium scouring conditions, the bed shear stress at the deepest scour region was found to be approximately equal to the critical Shields value for sediment motion on a flat bed. At other sloping regions in the scour hole, the bed shear stress was smaller than the Shields value.

INTRODUCTION

A large number of bridge failures due to abutment scour during flood events have been recorded and this is of great concern to engineers and scientists (Melville, 1992, Richardson and Richardson, 1993). Basically abutment scour is caused by the flow impinging on the abutment, thereby changing the flow direction and resulting in bed shear stress increase near the abutment nose. This causes the erosion of the streambed material and formation of a scour hole at the abutment. For abutment scour in two-stage channels, the problem is more complicated. The abutment may be located on the floodplain or extends into the main channel, and in either case, it blocks and diverts the floodplain flow towards the main channel resulting in a complex flow pattern and an increase in velocity which cause the scouring at the abutment.

Current abutment scour prediction techniques are not applicable to a wide range of field conditions, and the scour depth is often over-predicted. Over-predicting abutment scour may result in construction of unnecessary countermeasures or excessively deep foundations, adding significant costs to bridge construction and maintenance (Niehus, 1996). Most experimental studies of scour around abutments have been conducted in rectangular laboratory flumes in which the distributions of flow velocity and bed shear stress were considered uniform in the transverse direction (Laursen 1963, Gill 1972, Melville 1992, Lim 1997). Idealized experiments in

1 Research Fellow, Maritime Research Centre, School of Civil and Environmental Engineering, Nanyang Technological University, Nanyang Avenue, Singapore 639798, cglyu@ntu.edu.sg
2 Assoc. Prof., Maritime Research Centre, School of Civil and Environmental Engineering, Nanyang Technological University, Nanyang Avenue, Singapore 639798, csylim@ntu.edu.sg, ctansk@ntu.edu.sg

rectangular flumes are representative of flow around abutments in well-defined incised channels or abutments in wide braided rivers. However, real river channels are different from these idealized laboratory conditions, and often have compound cross-sections. Due to the presence of the abutment and the redistributions of flow and bed shear stress between the floodplain and the main channel, the downflows, turbulence, and vortices near the nose of the abutment are quite different compared to that in a rectangular channel.

A few studies have been conducted on abutment scour in two-stage channels, but only a limited number of experiments have been done on abutments that terminate at the end of the floodplain (Sturm and Janjua 1994, Dongol 1994, Melville 1995, Kouchakzadeh and Townsend 1997, Cardoso and Bettess 1999, Lim and Yu 2001). This paper presents results on the flow conditions and bed scouring vis-à-vis bed shear stress around an abutment terminating at the interface between the floodplain and the main channel (Case III (b) of Melville's classification, 1995).

EXPERIMENTAL SET-UP

The experiments were conducted in a large two-stage channel as shown in Figs. 1 and 2. The two-stage channel is 19 m long, 1.6 m wide and 0.75 m high, in which there is one floodplain situated on one side of the channel. The floodplain is 1 m wide, 0.6 m deep and is at 0.15 m above the main channel bed. Both the floodplain and the main channel have a bed slope of 1/1000. A honey comb was placed at the inlet of the flume in order to obtain a uniform inflow velocity. The velocity was measured using a three-dimensional Acoustic Doppler Velocimeter (ADV) and the bathymetry of scoured bed was measured using a point gauge. Both the ADV and the point gauge were attached to a carriage installed on top of the flume.

Fig. 1 View of two-stage flume

Two sediment recess tanks 3 m long each were installed on the floodplain and the main channel, respectively, at a distance 11 m from the flume inlet. The tank was filled with the test sediment. The one on the floodplain is 0.40 m deep and the other in the main channel is 0.25 m deep. A vertical-wall abutment model of 1 m length and 0.05 m wide was installed perpendicular to the channel wall in the floodplain and

placed at the center of the sediment tank, as shown in Fig.3. Other than the sediment recess tank, the floodplain and main channel beds were made of steel. Sediment particles with diameters of 5-10 mm were sprinkled uniformly on the approach section in order to simulate bed roughness.

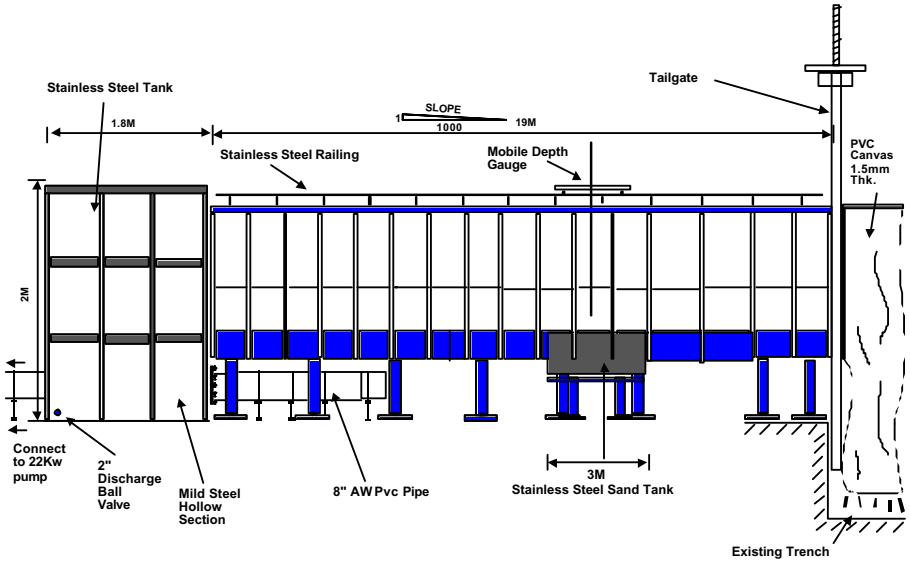

Fig. 2 Schematic sketch of flume

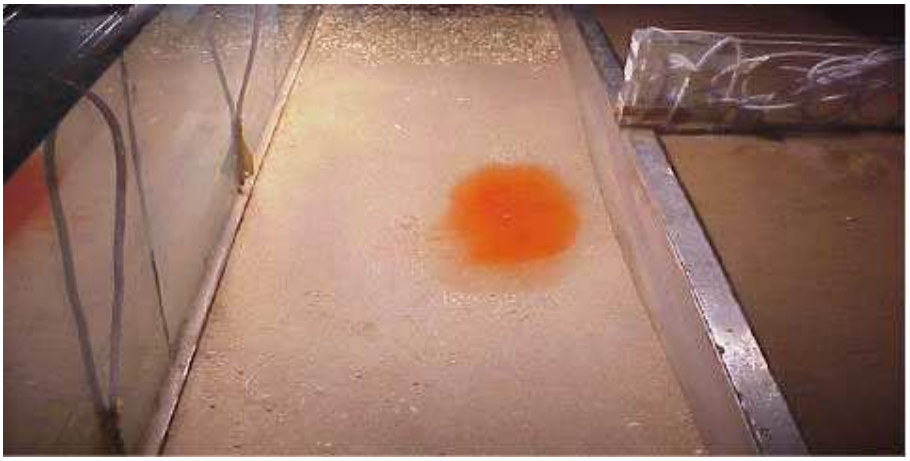

Fig. 3 View of abutment model

The sediment tanks were filled with uniform quartz sediment particles with a median diameter of 0.93 mm and a geometric sediment gradation of 1.17. The sediment beds were leveled to the same elevations as the floodplain and the main channel beds.

Each experiment was run for between one to three weeks, depending on the discharge, until the scouring process reached a static equilibrium state. Then, the pump was gently turned off and the water in the flume and the scour hole was slowly drained. When the scour hole was dry, the bathymetry of the scour hole was measured.

FLOW AROUND ABUTMENT

After the bathymetry measurement, the velocity field near the abutment was measured in the main channel using the ADV. The flow structure is shown in Fig. 4, based on extensive spatial velocity measurements around the abutment. The flow on the floodplain is diverted towards the main channel due to the abutment and converges with the main flow in the main channel. Spiral vortices can be seen generated at the upstream edge of the abutment nose. Viewing from the top, these spiral vortices rotate in an anticlockwise direction. Looking downstream, they roll in a clockwise direction. These vortices interfered and "blocked" the approach flow in the main channel. The blockage forced the approach flow to dive towards the bed with the formation of downflows on the right side of the spiral vortices. When the downflows pass under the vortices and then rise towards the water surface, large upflows (like an unsteady fountain) are generated on the left side of the spiral vortices (see Fig. 4). These upflow eddies in the main channel formed downstream of the abutment nose. The water surface elevation at the centers of the upflow eddies are generally higher than other places. The scales of the upflow eddies may be as large as the local flow depth. The upflow eddies eventually dispersed towards the floodplain. Fig. 4 also shows the formation of a large-scale flow circulation with a vertical axis at the corner behind the abutment.

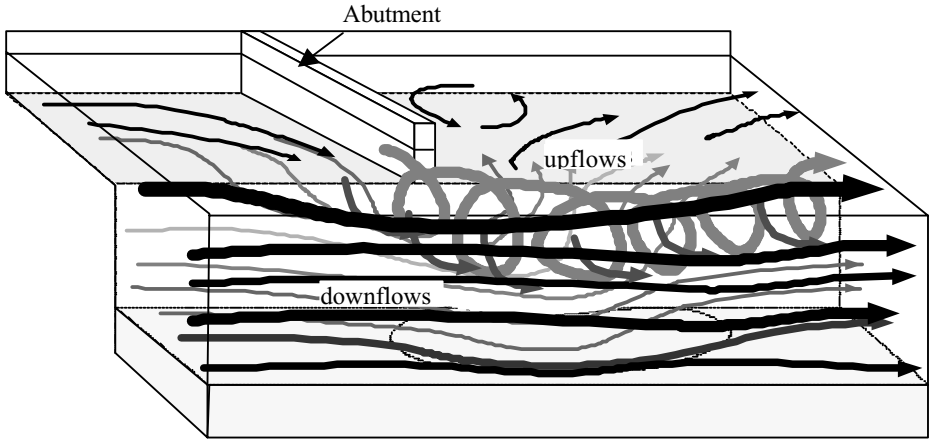

Fig. 4 Flow structure near abutment

The flow interactions and turbulence generated by the spiral vortices and upflow eddies are very strong, and these flow disturbances may be dangerous to navigation. At the core of the large-scale spiral vortices, the flow pattern is complex. At the edges of the spiral vortices boats may be sucked into the bottom by the diving downflows or turned over by the upflow eddies and spiral vortices. In order to investigate the path of the spiral vortices, floating objects were deliberately released upstream. The paths of the floating objects around and downstream of the abutment were recorded to obtain the centerlines of the spiral vortices. Fig. 5 shows the paths of the vortices as they spiraled from the abutment nose and their intrusion into the main channel. The 'intrusion' into the main channel is more severe as the flow discharge increases. The paths of the spiral vortices are similar to the trajectory of a projectile. The vortices generated at the upper edge of the abutment nose spiraled continuously into the main

channel and the maximum distance reached is approximately equal to the flow depth. The path then curves towards the floodplain region as the spiral proceed further downstream.

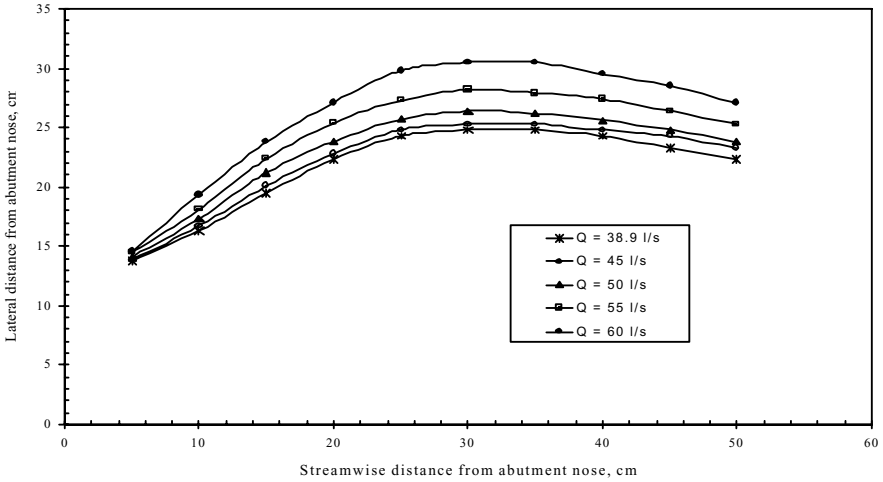

Fig. 5 Centerline location of large-scale vortices

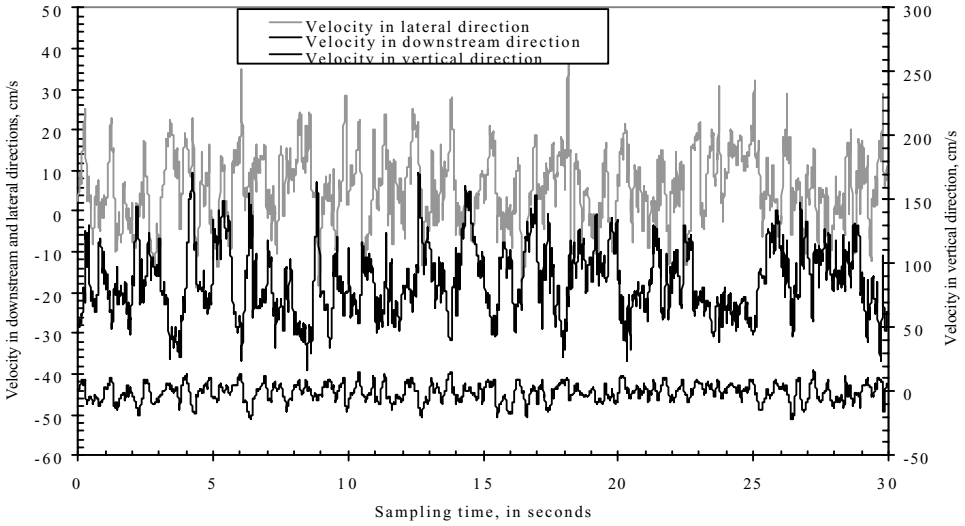

Fig. 6 Turbulence intensity in center of large-scale vortices

An example of the velocity fluctuation of the large scale vortex is shown in Fig. 6. The measurement was taken at a position 6.5 cm below the water surface in the main channel, 10 cm downstream of the abutment nose and 14 cm off the floodplain bank. The discharge was 60 l/s and flow depth in the main channel was 22.81 cm. The relative values of the average velocities in the lateral and vertical directions to the average velocity in the approach flow direction, $\overline{v}/\overline{u}$ and $\overline{w}/\overline{u}$, were about 0.31 and 0.06, respectively. However, the deviations of velocities in the three directions to the average velocity in the approach flow direction, $\sqrt{\overline{(u-\overline{u})^2}}/\overline{u}$, $\sqrt{\overline{(v-\overline{v})^2}}/\overline{u}$ and $\sqrt{\overline{(w-\overline{w})^2}}/\overline{u}$ were as high as 0.49, 0.52 and 0.41, respectively. The velocity measurements at other locations inside the large-scale vortices also show that the turbulence intensities are

high. This implies that the path of the large-scale vortices is a dangerous zone for navigation.

BED SHEAR STRESS DISTRIBUTION AROUND ABUTMENT

After the scour hole reached the equilibrium state, the velocity profiles near the bed at different locations within the scour hole were measured using the ADV. It was found that the velocity profiles complied with the logarithmic distribution. This is consistent with the findings of Ahmad and Rajaratnam (2000). Fig. 7 shows the velocity profiles at two locations with a discharge of 55 l/s. Fig. 7a shows a velocity dip near the water surface mainly because of the existence of the spiral vortices. The bed shear stress was obtained using a curve-fitting technique to the measured velocity profiles. The results indicated that the bed shear stress at the deepest location of the scour hole was very close to the critical shear stress for sediment motion on a flat bed, while at other places on the sloping part of the scour hole, the bed shear stresses were smaller than the critical shear stress on a flat bed. This may be due to the effect of the sloping bed on sediment motion. Figs. 8a to 8d show the bed shear stress distributions and scoured bed profiles for four different lateral sections in Run 9. The four locations in Figs. 8a to 8d are 24, 4, 12 and 32cm downstream of the abutment, respectively.

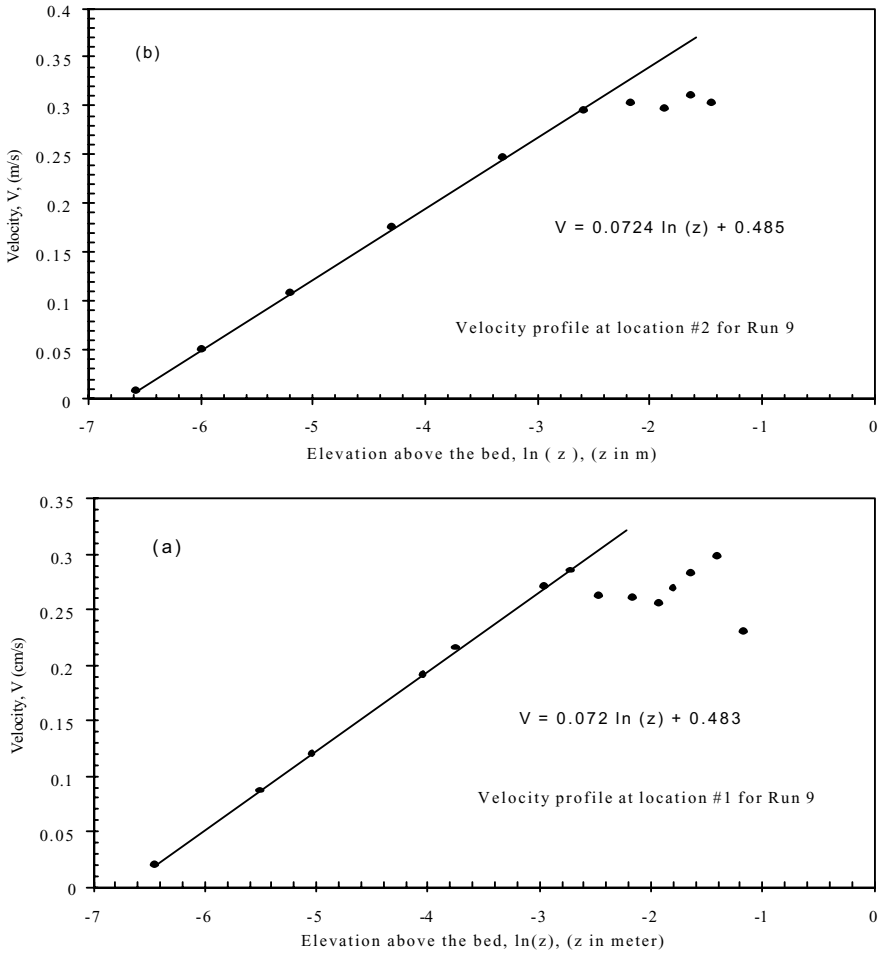

Fig. 7 Velocity profiles in scour hole for equilibrium scour

It was difficult to obtain the maximum bed shear stress near the abutment at the beginning of scouring because the rate of scouring was fast. However, it may be possible to obtain an estimate of the initial (time = 0) maximum bed shear stress near the abutment nose, t_{max} by interpolating the results of the shear measurements obtained at different scouring durations. The velocities at the planar location where the deepest scour hole occurred were measured every 30 minutes to obtain the bed shear stresses at different time interval. Fig. 9 shows the velocity profile for Run 9 after 85 minutes of scouring action. This maximum bed shear stress, t_{max}, was compared with the approach flat-bed shear stress, τ_{mc}, in the main channel (without abutment). As shown in Fig. 10, the interpolated ratios of t_{max}/τ_{mc} at time t = 0 were 3.8 and 3.6 for Runs 8 and 9, respectively.

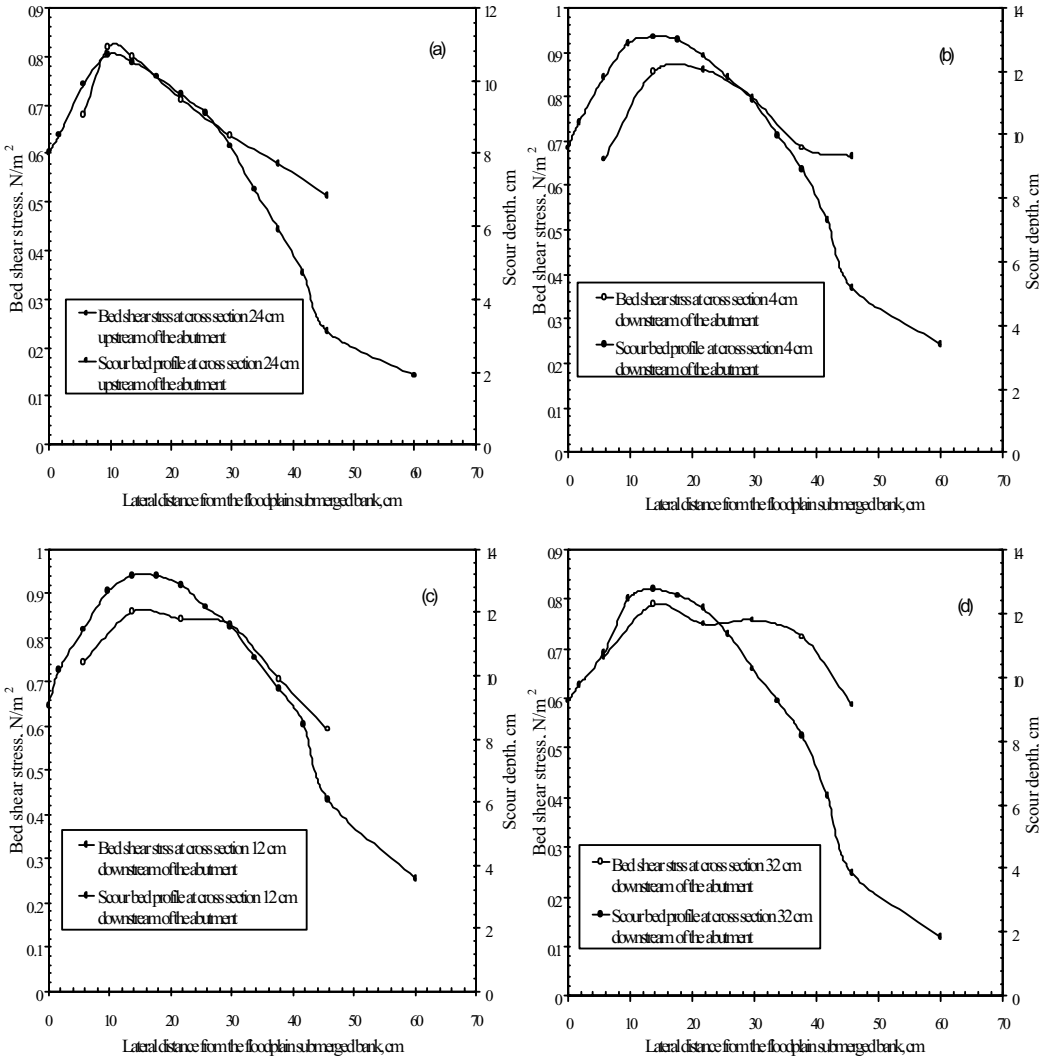

Fig. 8 Bed shear stress profiles in scour hole at equilibrium state for Run 9

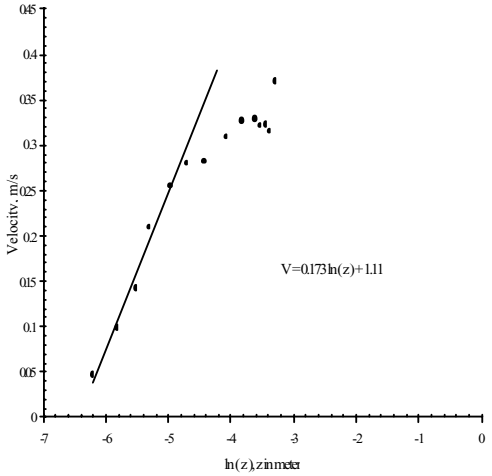

Fig. 9 Velocity profile after 85 minutes scouring

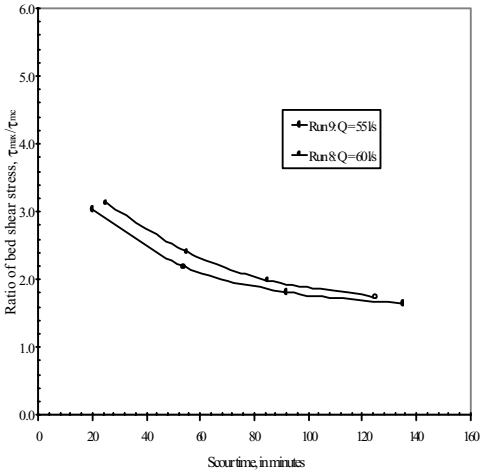

Fig. 10 Maximum bed shear stress decays with time

Fig. 11 shows the variation of t_{max}/τ_{mc} with approach discharge. The figure implies that t_{max}/τ_{mc} is dependent on the approach flow depth ratio and width ratio of the main channel and the floodplain. Fig. 11 shows that the maximum t_{max}/τ_{mc} = 3.8 was recorded for the maximum discharge, Q = 60 l/s used in this study. This value is comparable to that found by Ahmad and Rajaratnam (2000) on flow around abutments in rectangular channels. Their results show a maximum bed shear stress ratio amplification of about 3.63 times near the nose of the abutment. For circular bridge piers, the maximum bed shear stress ratio amplification was about 4.0 times at the nose of pier (Ettema 1980, Kothyari et al.; 1992). For flow around thin groynes, Rajaratnam and Nwachukwu (1983) found a fourfold increase in the bed shear stress near the tip of the groyne.

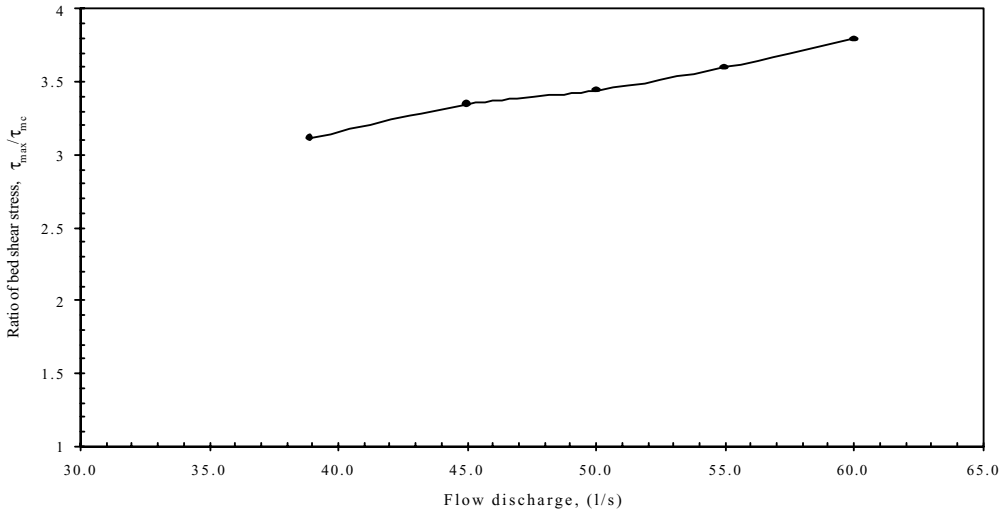

Fig. 11 Maximum bed shear stress in main channel against approach discharge

CONCLUSIONS

Experimental investigations demonstrate that the flow around an abutment in two-stage channels is complex, consisting of a spiral flow, an upflow and a downflow. The turbulence in the spiral flow and the upflow is strong and may be dangerous to navigation. The downflow is mainly responsible for bed scouring. The velocity profile around the abutment obeys the logarithmic law but the boundary layer thickness increases as the scouring process progresses.

The results show that the increase of the bed shear stress near the abutment location depends on the approach discharge. In the present test range, the maximum value of the bed shear stress amplification (t_{max}/τ_{mc}) before the scouring commences is 3.8 times near the nose of the abutment, and this corresponds approximately to the location in which the maximum scour depth was recorded. After the scouring reaches the equilibrium state, the dimensionless bed shear stress at the deepest position is equal to the critical Shields value for sediment motion, while at other places in the scour hole, the bed shear stress is smaller than the Shields value, probably due the effect of the sloping ground in these locations.

REFERENCES

Ahmad, F. and Rajaratnam N. (2000). "Observations on flow around bridge abutment." J. Engrg. Mech., ASCE , 126(1): 51-59.

Cardoso, A.H., and Bettess, R. (1999). "Effect of time channel geometry on scour at bridge abutments."*J. Hydr. Engrg*., ASCE, 125(4), 388-399.

Ettema, R.E. (1980). "Scour at bridge piers." Report No. 236. School of Engrg., The Univ. of Auckland, New Zealand.

Dongol, D.M.S. (1994). "Local scour at bridge abutments." Rep. No. 544, School of Engineering, University of Auckland, New Zealand.

Gill, M.A. (1972). "Erosion of sand beds around spur dikes." *J. Hyd. Div., ASCE,* 98(9), 1587-1602.

Kothyari, U.C., Garde, R.J. and Ranga Raju, K.G., (1992). "Temporal variation of scour around circular bridge piers." J. Hydr. Engrg. ASCE, 118(8), 1091-1106.

Kouchakzadeh, S., and Townsend, D.R. (1997). "Maximum scour depth at bridge abutments terminating in the floodplain zone." *Can. J. Civ. Eng*. 24: 996-1006.

Laursen, E.M. (1963). "An analysis of relief bridge scour." *J. Hydr. Div. ASCE,* 89(3), 93-118.

Lim, S.Y. (1997). "Equilibrium clear-water scour around an abutment." *J. Hydr. Engrg*., ASCE, 123(3), 237-243.

Lim, S.Y. and Yu, G, (2001). "Study on abutment scour in two-stage channel." Proceedings of XXIX IAHR Congress - 21st Century: The New Era for Hydraulics Research and its Applications, Beijing, China, Vol. II, Theme D, 16-21 Sept. 2001, pp. 8-13.

Melville, B.W. (1992). "Local scour at bridge abutments." *J. Hydr. Engrg*., ASCE, 118(4), 615-631.

Melville, B.W. (1995). "Bridge abutment scour in two-stage channels." *J. Hydr. Engrg*., ASCE, 121(12), 863-868.

Niehus, C.A., (1996), "Scour assessments and sediment-transport simulation for selected bridge sites in South Dakota." USGS, Water-Resources Investigations Report 96-4075.

Rajaratnam, N. and Nwachukwu, B.A. (1983). "Flow near groyne-like structure." J. Hydr. Engrg., ASCE, 109 (3), 463-480.

Richardson J.R. and Richardson E.V. (1993). "Discussion of local scour at bridge abutments." By B.W. Melville." *J. Hydr. Engrg*., ASCE, 119(9), 1069-1071.

Sturm, T.W., and Janjua, N.S. (1994). "Clear-water scour around abutments in floodplains." *J. Hydr. Engrg*., ASCE, 120(8), 956-972.